Journal of the American Heart Association

ORIGINAL RESEARCH

Relationship Between Optical Coherence Tomography–Derived In-Stent Neoatherosclerosis and the Extent of Lipid-Rich Neointima by Near-Infrared Spectroscopy and Intravascular Ultrasound: A Multimodal Imaging Study

Mitsuhiro Takeuchi ID, MD; Tomotaka Dohi ID, MD, PhD; Mitsuaki Matsumura, BS; Tatsuya Fukase, MD; Ryota Nishio, MD; Norihito Takahashi, MD, PhD; Hirohisa Endo ID, MD, PhD; Hiroki Nishiyama, MD; Shinichiro Doi, MD, PhD; Iwao Okai, MD; Hiroshi Iwata ID, MD, PhD; Shinya Okazaki, MD; Katsumi Miyauchi, MD, PhD; Hiroyuki Daida, MD, PhD; Tohru Minamino ID, MD, PhD

BACKGROUND: In-stent restenosis, especially for neoatherosclerosis, is a major concern following percutaneous coronary intervention. This study aimed to elucidate the association of features of in-stent restenosis lesions revealed by optical coherence tomography (OCT)/optical frequency domain imaging (OFDI) and the extent of lipid-rich neointima (LRN) assessed by near-infrared spectroscopy (NIRS) and intravascular ultrasound, especially for neoatherosclerosis.

METHODS AND RESULTS: We analyzed patients undergoing percutaneous coronary intervention for in-stent restenosis lesions using both OCT/OFDI and NIRS–intravascular ultrasound. OCT/OFDI-derived neoatherosclerosis was defined as lipid neointima. The existence of large LRN (defined as a long segment with 4-mm maximum lipid core burden index ≥400) was evaluated by NIRS. In 59 patients with 64 lesions, neoatherosclerosis and large LRN were observed in 17 (26.6%) and 21 lesions (32.8%), respectively. Naturally, large LRN showed higher 4-mm maximum lipid core burden index (median [interquartile range], 623 [518–805] versus 176 [0–524]; $P<0.001$). In OCT/OFDI findings, large LRN displayed lower minimal lumen area (0.9±0.4 versus 1.3±0.6 mm^2; $P=0.02$) and greater max lipid arc (median [interquartile range], 272° [220°–360°] versus 193° [132°–247°]; $P=0.004$). In the receiver operating characteristic curve analysis, 4-mm maximum lipid core burden index was the best predictor for neoatherosclerosis, with a cutoff value of 405 (area under curve, 0.92 [95% CI, 0.83–1.00]). In multivariable logistic analysis, only low-density lipoprotein cholesterol (odds ratio, 1.52 [95% CI, 1.11–2.08]) was an independent predictor for large LRNs.

CONCLUSIONS: NIRS-derived large LRN was significantly associated with neoatherosclerosis by OCT/OFDI. The neointimal characterization by NIRS–intravascular ultrasound has potential as an alternative method of OCT/OFDI for in-stent restenosis lesions.

Key Words: in-stent restenosis ■ near-infrared spectroscopy ■ neoatherosclerosis ■ optical coherence tomography ■ optical frequency domain imaging

---

JAHA is available at: www.ahajournals.org/journal/jaha

CLINICAL PERSPECTIVE

What Is New?

- The present study aimed to elucidate the relationship between the distribution of lipids in in-stent restenosis lesions, as assessed by near-infrared spectroscopy, and neoatherosclerosis diagnosed by optical coherence tomography/optical frequency domain imaging, and to clarify the clinical risk factors for the development of large lipid-rich neointima.
- Near-infrared spectroscopy–derived 4-mm maximum lipid core burden index showed highest diagnostic ability for neoatherosclerosis detected by optical coherence tomography/optical frequency domain imaging.
- High low-density lipoprotein cholesterol level was an independent clinical risk factor for large lipid-rich neointima in patients undergoing percutaneous coronary intervention.

What Are the Clinical Implications?

- The neointimal characterization by near-infrared spectroscopy–intravascular ultrasound has the potential to be an alternative method of optical coherence tomography/optical frequency domain imaging, and the cutoff value of 4-mm maximum lipid core burden index ≥400 was useful not only in native coronary artery lesions but also in-stent restenosis lesions.
- Because the higher low-density lipoprotein cholesterol was significantly associated with large lipid-rich neointima, a more restrictive lipid-lowering treatment may be needed for patients after stent implantation.

Nonstandard Abbreviations and Acronyms

DES	drug-eluting stent
ISR	in-stent restenosis
LRN	lipid-rich neointima
maxLCBI$_{4mm}$	4-mm maximum lipid core burden index
NIRS	near-infrared spectroscopy
OFDI	optical frequency domain imaging

Percutaneous coronary intervention (PCI) with stent implantation is a common procedure for the treatment of coronary artery disease. In-stent restenosis (ISR) results from arterial damage with subsequent neointimal tissue proliferation after stent implantation.[1] The use of drug-eluting stents (DESs) has greatly reduced the proportion of restenosis compared with the bare-metal stents by suppressing acute-phase excessive neointima proliferation.[2] However, impaired healing of the endothelium by DESs promotes lipid deposition within the neointima, leading to the development of neoatherosclerosis,[3,4] which is associated with worse clinical outcomes.[5,6] The cause and risk factors of neoatherosclerosis have not yet been fully clarified. Therefore, ISR remains a major concern in the field of current coronary intervention.

Originally described in pathological studies, neoatherosclerosis has increasingly been detected in intracoronary image studies.[7,8] Optical coherence tomography (OCT) and optical frequency domain imaging (OFDI) have the ability to provide high-resolution images and divide neointimal tissue into several patterns that correlate with different histological substrates, including neoatherosclerosis.[9,10] However, OCT/OFDI requires the evacuation of blood from the vessel using contrast media or low-molecular-weight dextran, which limits its use in situations such as renal dysfunction. In contrast, the combination of near-infrared spectroscopy (NIRS) and intravascular ultrasound (IVUS) in a single catheter allows for assessment of plaque composition in both quantitative evaluation of lipids by NIRS[11,12] and qualitative characteristics by IVUS,[13] without the evacuation of blood. The approval for NIRS-IVUS from the US Food and Drug Administration is based on the results of the landmark Lipid-Rich Plaque study,[14] which demonstrated the ability of NIRS-IVUS in evaluating plaque vulnerabilities in native coronary arteries. Given its ability to detect coronary lipid-rich plaques, NIRS-IVUS has been proposed as an alternative method of OCT/OFDI for detecting neoatherosclerosis; however, to date, only limited data are evaluated on the ability of NIRS-IVUS for detecting neoatherosclerosis.[15,16] Thus, the aim of the present study was to evaluate the relationship between the distribution of lipids in ISR lesions as assessed by NIRS and neoatherosclerosis diagnosed by OCT/OFDI and to clarify the clinical risk factors for the development of large lipid-rich neointima (LRN).

METHODS

The data that support the findings of this study are available from the corresponding author on reasonable request.

Study Population and Data Collection

In this prospective, single-center, observational study, we enrolled consecutive patients who underwent PCI for ISR lesions using both OCT/OFDI and NIRS-IVUS at Juntendo University Hospital (Tokyo, Japan) from January 2018 to August 2021. The ISR lesion was defined as a lesion with diameter of stenosis of

>50% within either the stented segment or a 5-mm segment proximal or distal to the stent edge by visual assessment.[17] The exclusion criteria were as follows: (1) patients who did not receive preintervention OCT/OFDI or NIRS-IVUS pullback and (2) patients for whom adequate NIRS analysis could not be obtained. The procedures were performed according to the current standard clinical guidelines. In all cases, the intervention strategy of whether to use DES or drug-coating balloon was at the discretion of the operator. Written informed consent for the present study was obtained from all patients before PCI. This study was conducted in accordance with the Declaration of Helsinki and with the approval of the institutional review board of Juntendo University (institutional review board identifier: 17-170).

Demographic data, coronary risk factors, and medication information were collected from our institutional database. Blood samples were collected before the procedure.

OCT/OFDI Imaging and Analysis

The OCT/OFDI images were acquired using frequency-domain OCT systems (OCT: Dragonfly JP catheter and ILUMIEN OPTIS system, Abbott Vascular, IL; OFDI: Fast View catheter and LUNAWAVE system, Terumo, Tokyo, Japan). A detailed description of the measurements and quantitative analyses of OCT/OFDI is provided in Data S1.

The qualitative morphological appearance of the neointima was assessed at the minimal lumen area (MLA) site. In the present study, we used a novel OCT/OFDI classification of in-stent neointima that aimed to classify most ISR lesions easily and certainly with a higher degree of reproducibility based on the previous studies.[10,18] To reflect histological substrates, in-stent neointima tissue characteristics were classified into 4 groups as follows: (1) homogeneous neointima pattern; (2) heterogeneous neointima with layered pattern; (3) heterogeneous neointima without layered pattern; and (4) neoatherosclerosis pattern (Figure 1 and Data S1). The criteria for the diagnosis of neoatherosclerosis were lesion with lipid neointima. Lipid neointima was defined as having signal-poor regions with diffuse borders and high attenuation, such that stent struts behind the neointima were invisible. The arc of lipid neointima was also analyzed.

NIRS-IVUS Imaging and Analysis

NIRS-IVUS imaging was performed after OCT/OFDI image acquisition using a commercially available system (TVC Imaging System or Makoto Imaging System, Infraredx, MA). A detailed description of the acquisition and measurement of NIRS-IVUS with definitions is provided in Data S1. In the present study, lipid core burden index was calculated for every 4-mm segment within the stent. The 4-mm maximum lipid core burden index ($maxLCBI_{4mm}$) was defined as the maximum lipid core burden index within any 4-mm-long culprit segment. Large LRN was defined as an in-stent lipid-rich plaque having a $maxLCBI_{4mm}$ ≥400.[19,20]

A detailed description of the measurements for quantitative analyses of IVUS is also provided in Data S1. Offline analyses of both OCT/OFDI
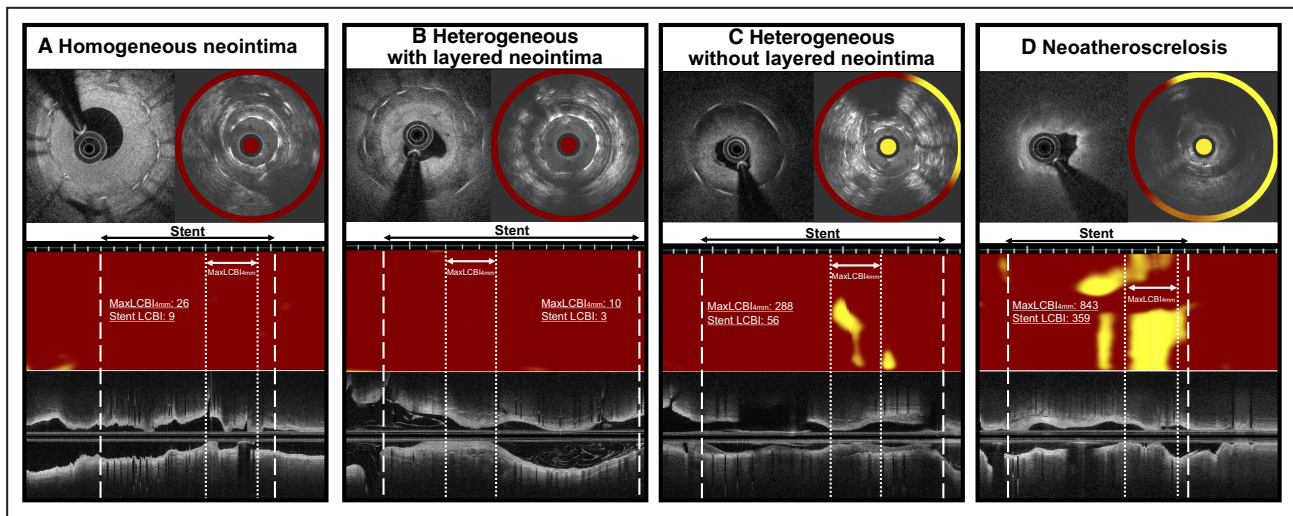
Figure 1. Classification of in-stent neointima patterns evaluated by optical coherence tomography/optical frequency domain imaging. In-stent neointima tissue characteristics were classified into 4 groups.

A, Homogeneous neointima pattern: signal-rich regions with low attenuation. **B**, Heterogeneous with layered neointima pattern: one with layers having different optical properties (ie, an adluminal high-scattering layer and an abluminal low-scattering layer). **C**, Heterogeneous without layered neointima pattern: one with focally changing optical properties with low attenuation. **D**, Neoatherosclerosis pattern: a signal-poor region with diffuse borders. LCBI, lipid core burden index; and $MaxLCBI_{4mm}$, 4-mm maximum LCBI.

and NIRS-IVUS in all imaged segments were performed using computerized planimetry software (QIVUS, Medis Medical Imaging System, Leiden, the Netherlands). The analyses of all images required the agreement of 2 observers (M.T. and T.D.) who were blinded to all clinical and procedural characteristics. When there was discordance between 2 readers, consensus reading was obtained from a third independent investigator (M.M.).

Statistical Analysis

All data were analyzed using JMP for Windows version 14.3 (SAS Institute, Cary, NC). Quantitative data are presented as mean±SD or median (interquartile range), whereas categorical variables are presented as frequencies. Continuous variables between groups were compared using the unpaired t test or Mann-Whitney U test. Categorical variables across the groups were compared using the χ^2 or Fisher exact test, and differences between the neointima types were assessed using 1-way ANOVA. A 2-tailed $P<0.05$ was considered statistically significant. Baseline characteristics were compared between 2 groups: large LRN and nonlarge LRN. Receiver operating characteristic curves were used to determine the best cutoff values for predicting neoatherosclerosis and large LRN. Logistic regression analysis was used to calculate the odds ratio (OR) of the large LRN using all patient background factors. Variables with $P<0.05$ on univariable logistic regression

analysis were included in the multivariable logistic regression analysis.

RESULTS

Baseline Clinical Characteristics

During the study period, 61 patients with 66 ISR lesions underwent PCI using both OCT/OFDI and NIRS-IVUS imaging. Among them, 2 patients were excluded as 1 did not receive preprocedural NIRS-IVUS pullback, and an adequate NIRS chemogram could not be obtained from the other. Ultimately, we analyzed 59 patients with 64 lesions (bare-metal stent: 7 cases [10.9%]; first-generation DES: 18 cases [28.1%]; and second-generation DES: 39 cases [60.9%]).

Comparison Between the Lesions With NIRS-Derived Large LRN Versus Nonlarge LRN

Twenty-one lesions (32.8%) were identified as large LRN. Patients with large LRN showed lower body mass index (23.7±2.1 versus 25.9±3.6 kg/m^2; $P=0.01$) and higher low-density lipoprotein cholesterol (LDL-C) (86.8±25.2 versus 70.5±17.5 mg/dL; $P=0.004$) than those with nonlarge LRN (Table 1). There were no significant differences in the lesion characteristics and angiographic data between the 2 groups. In terms of the treatment strategy, DESs were implanted more

Table 1. Clinical Characteristics of Patients

	Overall (n=59)	Patients with large LRN (n=20)	Patients with nonlarge LRN (n=39)	P value
Baseline characteristic				
Age, y	69.8±10.0	70.8±9.1	69.3±10.5	0.71
Men, n (%)	49 (83.1)	17 (85.0)	32 (82.1)	0.77
BMI, kg/m^2	25.1±3.4	23.5±1.9	25.9±3.7	0.01
Hypertension, n (%)	49 (83.1)	15 (75.0)	34 (87.2)	0.24
Diabetes, n (%)	30 (50.9)	10 (50.0)	20 (51.3)	0.93
Dyslipidemia, n (%)	57 (96.6)	19 (95.0)	38 (97.4)	0.63
Current smoker, n (%)	5 (8.5)	0 (0.0)	5 (12.8)	0.16
Serum creatinine, mg/dL	0.91 (0.69–1.10)	0.87 (0.68–1.05)	0.96 (0.74–1.11)	0.25
TC, mg/dL	148.6±29.2	158.8±36.3	144.0±24.6	0.08
LDL-C, mg/dL	75.7±21.8	86.4±25.7	69.9±17.0	0.005
HDL-C, mg/dL	45.1±12.5	45.9±10.6	44.6±13.5	0.73
Triglycerides, mg/dL	107 (82–194)	127 (81–211)	100 (85–194)	0.51
HbA1c, %	6.4±0.8	6.4±0.8	6.4±0.9	0.79
Medication, n (%)				
Statin	52 (88.1)	17 (85.0)	35 (89.7)	0.59
High-intensity statin	15 (25.4)	3 (15.0)	12 (30.8)	0.22
Ezetimibe, n (%)	20 (33.9)	8 (40.0)	12 (30.8)	0.48

Data are given as mean±SD or median (interquartile range), unless otherwise indicated. The doses of high-intensity statin were defined as rosuvastatin of 10 to 20 mg/d, atorvastatin of 20 mg/d, or pitavastatin of 4 mg/d, according to the approved doses in Japan. BMI indicates body mass index; HbA1c, hemoglobin A1c; HDL-C, high-density lipoprotein cholesterol; LDL-C, low-density lipoprotein cholesterol; LRN, lipid-rich neointima; and TC, total cholesterol.

frequently in large LRN lesions (47.6% versus 20.9%; P=0.04), whereas drug-coating balloon was performed in more frequently in nonlarge LRN lesions (52.4% versus 79.1%; P=0.04) (Table 2 and Table S1). All procedures were completed with thrombolysis in myocardial infarction 3 flow, so the difference was not observed for each lesion.

In the OCT/OFDI findings, the large LRN showed a lower MLA (0.9±0.4 versus 1.3±0.6 mm^2; P=0.02) and a greater maximum lipid arc (272° [220°–360°] versus 193° [132°–247°]; P=0.004) compared with that of nonlarge LRN. In NIRS analysis, the classification was based on maxLCBI$_{4mm}$; so naturally, the large LRN showed a higher maxLCBI$_{4mm}$ (623 [518–805] versus 176 [0–524]; P<0.001) than nonlarge LRN. IVUS findings did not show a significant difference between the 2 groups, except for smaller stent areas at MLA sites (5.8±1.4 versus 6.9±2.1 mm^2; P=0.02) and higher proportions of attenuated neointima (14 [66.7%] versus 6 [13.0%]; P<0.001) in the large LRN than nonlarge LRN (Table 3 and Table S1).

OCT-Derived In-Stent Neointimal Tissue Pattern

Of 64 ISR lesions, 20 (31.3%) had homogeneous neointima, 9 (14.1%) had heterogeneous with layered neointima, 18 (28.1%) had heterogeneous without layered neointima, and 17 (26.6%) had neoatherosclerosis. Neoatherosclerosis showed significantly higher maxLCBI$_{4mm}$ than nonneoatherosclerosis (623 [528–821] versus 46 [0–236]; P<0.001) (Figure 2). Conversely, there were no significant differences in maxLCBI$_{4mm}$ among 3 types of neointimas: homogeneous neointima (55 [0–275]), heterogeneous with layered neointima

(0 [0–78]), and heterogeneous without layered neointima (87 [0–243]) (P=0.10).

Diagnostic Ability of NIRS-IVUS to Identify OCT/OFDI-Derived Neoatherosclerosis

The receiver operating characteristic curve analysis of the neoatherosclerosis revealed that the best cutoff values to diagnose neoatherosclerosis were a maxLCBI$_{4mm}$ >405, an OCT/OFDI-derived maximum lipid arc >218°, and an IVUS-derived percentage neointima hyperplasia at the MLA site >85%. The maxLCBI$_{4mm}$ value had the highest predictive value for neoatherosclerosis (area under curve [AUC], 0.92 [95% CI, 0.83–1.00]; P<0.001) than the OCT/OFDI-derived maximum lipid arc (AUC, 0.80 [95% CI, 0.65–0.94]; P=0.001), whereas IVUS-derived percentage neointima hyperplasia at the MLA site could not show the accuracy of diagnostic ability for neoatherosclerosis (AUC, 0.57 [95% CI, 0.40–0.74]; P=0.42) (Figure 3 and Table S2).

Clinical Predictors of the Extent of Large LRN

Univariable logistic regression analysis revealed that the higher LDL-C per 10 mg/dL increase (OR, 1.47 [95% CI, 1.10–1.96]; P=0.004) and body mass index <25 kg/m^2 (OR, 0.32 [95% CI, 0.10–0.97]; P=0.04) were significantly associated with large LRN. After adjustment for other covariates, only higher LDL-C was an independent predictor for large LRN (adjusted OR, 1.52 [95% CI, 1.11–2.08]; P=0.003) (Table 4). The optimal cutoff value for identifying the

Table 2. Procedure Characteristics of Lesions

Variable	Overall (n=64)	Large LRN (n=21)	Nonlarge LRN (n=43)	*P* value
Clinical presentation at stent implantation, n (%)				0.33
ACS	19 (30.2)	8 (38.1)	11 (26.2)	
Stable CAD	44 (69.8)	13 (61.9)	31 (73.8)	
Time from stent implant, y	5.8 (1.0–12.4)	6.5 (3.3–10.1)	4.8 (0.9–12.5)	0.80
>6.0y, n (%)	31 (49.2)	11 (55.0)	20 (46.5)	0.53
Stent diameter, mm	2.75 (2.5–3.0)	2.5 (2.5–2.75)	2.75 (2.5–3.0)	0.57
Stent length, mm	26.6±8.7	25.1±8.7	27.3±8.7	0.36
Stent type, n (%)				0.81
BMS	7 (10.9)	2 (9.5)	5 (11.6)	
First-generation DES	18 (28.1)	7 (33.3)	11 (25.6)	
Second-generation DES	39 (60.9)	12 (57.1)	27 (62.8)	
ACS presentation at restenosis, n (%)	10 (15.6)	5 (23.8)	5 (11.6)	0.28
Treatment, n (%)				
DCB	45 (70.3)	11 (52.4)	34 (79.1)	0.04
DES	19 (29.7)	10 (47.6)	9 (20.9)	0.04

Data are given as mean±SD or median (interquartile range), unless otherwise indicated. ACS indicates acute coronary syndrome; BMS, bare-metal stent; CAD, coronary artery disease; DCB, drug-coating balloon; DES, drug-eluting stent; and LRN, lipid-rich neointima.

Table 3. Imaging Characteristics of Lesions

Variable	Overall (n=64)	Large LRN (n=21)	Nonlarge LRN (n=43)	*P* value
OCT/OFDI findings				
MLA, mm^2	1.2±0.6	0.9±0.4	1.3±0.6	0.02
Stent area at MLA site, mm^2	5.5±1.8	4.9±1.1	5.8±2.0	0.06
NIH at MLA site, %	76.9±9.9	78.9±8.6	75.9±10.4	0.26
Maximum lipid arc, °	230 (143–290)	272 (220–360)	193 (132–247)	0.004
NIRS findings				
MaxLCBI$_{4mm}$	176 (0–524)	623 (518–805)	26 (0–205)	<0.001
IVUS findings				
MLA, mm^2	2.1±0.9	1.9±0.7	2.2±1.0	0.28
Vessel area at MLA site, mm^2	15.3±4.3	14.4±3.3	15.7±4.6	0.28
Stent area at MLA site, mm^2	6.5±2.0	5.8±1.4	6.9±2.1	0.02
NIH at MLA site, %	65.6±15.7	64.6±15.1	66.1±16.1	0.73
Attenuation, n (%)	20 (31.3)	14 (66.7)	6 (14.0)	<0.001

Data are given as mean±SD or median (interquartile range), unless otherwise indicated. IVUS indicates intravascular ultrasound; LRN, lipid-rich neointima; MaxLCBI$_{4mm}$, 4-mm maximum lipid core burden index; MLA, minimal lumen area; NIH, neointima hyperplasia; NIRS, near-infrared spectroscopy; OCT, optical coherence tomography; and OFDI, optical frequency domain imaging.

large LRN for LDL-C was >66 mg/dL (OR, 5.53 [95% CI, 1.38–22.3]; *P*=0.02).

DISCUSSION

The major findings of this study were as follows: (1) almost 30% of patients with ISR had an NIRS-derived large LRN with a lower MLA and a greater maximum lipid arc by OCT/OFDI; (2) OCT/OFDI-derived neoatherosclerosis had a higher maxLCBI$_{4mm}$, which

substantiates that the maxLCBI$_{4mm}$ threshold to predict neoatherosclerosis was 405; and (3) in the multivariable logistic regression analysis, LDL-C was the best predictor of large LRN.

NIRS is a spectroscopic method with the ability to quantify the lipid content of intracoronary plaques with high accuracy based on autopsy studies.[11,12] Quantifying plaque lipid by NIRS could predict further cardiovascular events, as recently demonstrated by the Lipid-Rich Plaque Study[14] and PROSPECT (A Prospective Natural
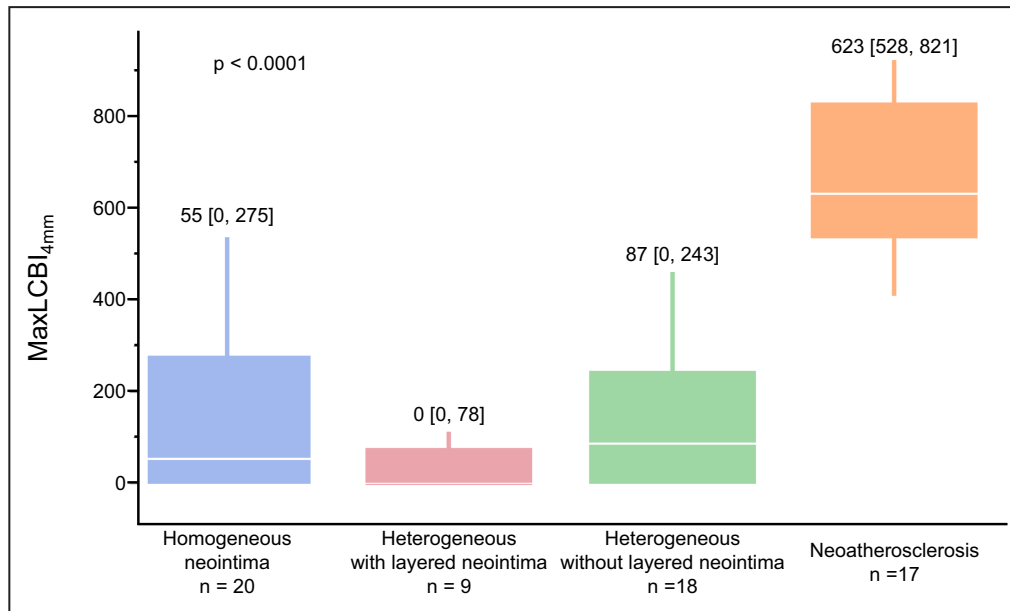
Figure 2. Relationship between the extent of lipid-rich neointima (MaxLCBI$_{4mm}$) by near-infrared spectroscopy and in-stent neointima characteristics by optical coherence tomography/optical frequency domain imaging.
Neoatherosclerosis showed highest MaxLCBI$_{4mm}$ (623 [528–821]) than homogeneous neointima (55 [0–275]), heterogeneous with layered neointima (0 [0–78]), and heterogeneous without layered neointima (87 [0–243]) (*P*<0.001). MaxLCBI$_{4mm}$ indicates 4-mm maximum lipid core burden index.
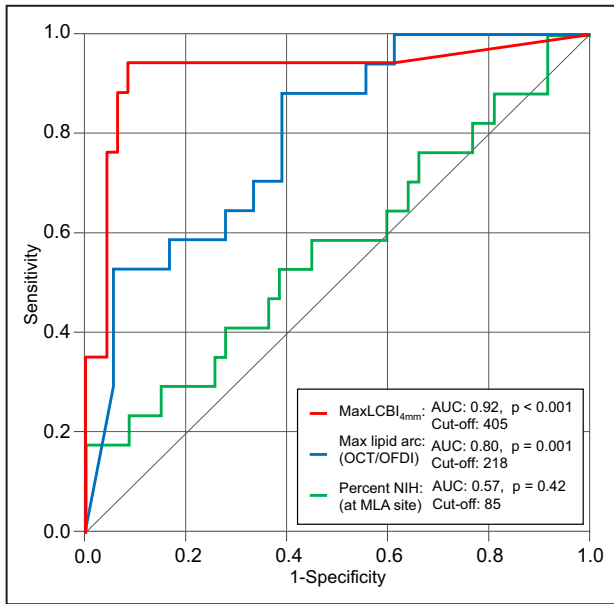
Figure 3. Receiver operating characteristic curve for predicting neoatherosclerosis.
The MaxLCBI$_{4mm}$ by near-infrared spectroscopy was the best parameter for predicting neoatherosclerosis, with a cutoff value of 405. AUC indicates area under the curve; Max, maximum; MaxLCBI$_{4mm}$, 4-mm maximum lipid core burden index; MLA, minimal lumen area; NIH, neointima hyperplasia; OCT, optical coherence tomography; and OFDI, optical frequency domain imaging.

History of Coronary Atherosclerosis) II study.[21] Zanchin et al also revealed the relationship between NIRS-detected lipid-rich plaque in native coronary arteries and their morphological plaque characteristics using OCT and IVUS.[22] In that study, lesions with maxLCBI$_{4mm}$ >400 showed greater lipid arc than lesions with maxLCBI$_{4mm}$ ≤400, which is consistent with our study, whereas MLA was comparable between the 2 groups. In the coronary artery, expansive remodeling works to maintain the lumen area for compensating plaque progression. In contrast, in ISR lesions, expansive

remodeling might not be able to compensate for a narrowing lumen caused by atherogenic progression within the neointima, as the outer circumference of the lesion is covered with the metallic stent. Araki et al reported that lumen volume decreased equally in ISR lesions, although the change of out-stent plaque volume index, which represents expansive remodeling, was significantly higher in neoatherosclerosis lesions compared with that in nonneoatherosclerosis lesions.[23] In ISR lesions, the quantitative assessment of lipids by NIRS might have the potential to reflect the degree of stenosis than the native coronary lesions.

ISR lesions have a variety of histological characterizations, and the specific imaging patterns of OCT/OFDI are reported to correlate with specific histological findings.[10] In the present study, we classified OCT/OFDI findings into 4 groups expected to reflect the vulnerabilities of neointimal tissue. Similar to the arteriosclerosis in the native arteries, neoatherosclerosis has pathological characteristics, such as foamy macrophage infiltration and necrotic core plaque formation with or without thin fibrous caps.[3] The cutoff value of maxLCBI$_{4mm}$ for detecting neoatherosclerosis was 405. This was nearly equal to the value used in our study for the definition of large LRN, which was based on previous studies that investigated lipid plaques in the native coronary arteries.[14,20,22] However, the thresholds for maxLCBI$_{4mm}$ to detect neoatherosclerosis in the present study were higher than the thresholds (>144) to detect thin-cap neoatherosclerosis (neoatherosclerosis with fibrous cap thickness <65 μm) in a previous study.[16] This discrepancy may be the result of differences in the definitions used for neoatherosclerosis. The report they cited as the criteria for OCT imaging classifications derived 3 categories of atherosclerosis, such as lipid, fibrous, and fibrocalcific.[24] In contrast, the fibrous neointima in the present study was categorized into not neoatherosclerosis but homogeneous neointima, which showed lower maxLCBI$_{4mm}$ than

Table 4. Logistic Regression Analysis for Large LRN

Variable	Univariable logistic analysis			Multivariable logistic analysis		
	OR	95% CI	*P* value	OR	95% CI	*P* value
LDL-C (per 10-mg/dL increase)	1.47	1.10–1.96	0.004	1.52	1.11–2.08	0.003
Men	1.17	0.27–5.05	0.84			
BMI >25 kg/m²	0.32	0.10–0.97	0.04	0.29	0.09–1.02	0.05
Implanted duration >6 y	1.41	0.48–4.08	0.53			
Stent type						
BMS	1.00 (Reference)	…				
First-generation DES	1.59	0.24–10.6	0.63			
Second-generation DES	1.11	0.19–6.56	0.91			
ACS at stent implantation	1.73	0.57–5.30	0.33			

ACS indicates acute coronary syndrome; BMI, body mass index; BMS, bare-metal stent; DES, drug-eluting stent; LDL-C, low-density lipoprotein cholesterol; LRN, lipid rich neointima; and OR, odds ratio.

neoatherosclerosis. Therefore, differences of the definition of neoatherosclerosis among the studies might have resulted in the lower cutoff values for neoatherosclerosis of the previous study.

The previous study demonstrated that the neoatherosclerosis showed the higher $maxLCBI_{4mm}$ than other types of neointimas. Of note, $maxLCBI_{4mm}$ has shown to be the best predictor of neoatherosclerosis with an optimal cutoff value of >405 and a higher AUC of 0.92 than OCT/OFDI-derived maximal lipid arc (AUC, 0.80) and IVUS-derived percentage neointima hyperplasia at the MLA site (AUC, 0.57). The previous studies showed that most culprit lesions in ST-segment–elevation myocardial infarction[19] and nonculprit lesions in acute coronary syndrome[22] contain a lipid-rich plaque with a $maxLCBI_{4mm}$ >400, a threshold that emerged as an accurate predictor of the presence of a vulnerable plaque by means of OCT. The consistency between the aforementioned studies and ours suggests that the $maxLCBI_{4mm}$ threshold of >400 is an expression and marker of not only coronary plaque but also in-stent neointima vulnerability. This is of clinical importance: although OCT/OFDI analysis (ie, measuring minimal lumen area, percentage neointima hyperplasia, and lipid arc) is complex, is time-consuming, and often requires the expertise of a dedicated core laboratory with experienced analysts, especially in lesions with calcification, the assessment of the $maxLCBI_{4mm}$ value can be derived easily and instantaneously in the catheterization laboratory. Therefore, NIRS-IVUS can risk stratify the patient ad hoc and provides a reliable assessment of neointima vulnerability, consistent with the acknowledged OCT/OFDI high-risk criteria.

Despite several studies focused on the clinical features of neoatherosclerosis, there have been no risk factors established for neoatherosclerosis progression to date. Kuroda et al reported that higher LDL-C, in addition to C-reactive protein levels, were independent predictors for neoatherosclerosis, which was also significantly associated with large LRN in the present study.[5] As previously reported, atherosclerotic plaque progression is directly related to higher LDL-C levels,[25,26] and there may be a similar relationship between the extent of LRN and LDL-C. For lipid-lowering therapy, a previous NIRS-IVUS study showed that the lipid core burden index of nonculprit plaque was significantly decreased, resulting from LDL-C reduction by proprotein convertase subtilisin-kexin type 9 inhibitor.[27] Moreover, the OCT study revealed that lipid-lowering therapy increases fibrous components of neointima in ISR.[28] Taken together, aggressive LDL-C reduction therapies, such as high-intensity statin treatments and proprotein convertase subtilisin-kexin type 9 inhibitor treatments, could lead to lipid reduction of LRN that results in stabilization.

The present study had some limitations. First, we included only patients with ISR undergoing PCI with both OCT/OFDI and NIRS-IVUS. Although we performed OCT/OFDI as much as possible using low-weight molecular dextran in patients with renal dysfunction, there was a possibility of selection bias. Second, we did not validate the OCT/OFDI and NIRS-IVUS findings with histological findings, and thus the regions identified as neoatherosclerosis and large LRN were not confirmed as containing atherosclerotic changes within the neointima. Third, because OCT/OFDI imaging during the index PCI was not performed, information on underlying plaque morphology was not available. Fourth, morphological assessment by OCT/OFDI was performed at MLA sites only, and several cases contained ≥2 neointima patterns in the total stented segment. Therefore, further detailed qualitative assessment for each type of neointima is needed. Finally, we defined large LRN as a $maxLCBI_{4mm}$ ≥400, but it cannot be certain whether this large $maxLCBI_{4mm}$ value originated from the tissue within the stent.[29]

The present study demonstrated an important relationship between NIRS-determined LRNs and neoatherosclerosis by OCT/OFDI in patients who had ISR. We also confirmed that in-stent NIRS-IVUS assessment could be useful to differentiate neoatherosclerosis from nonneoatherosclerosis lesions, and that a threshold $maxLCBI_{4mm}$ of ≥400 was clinically suitable. Considering that a higher LDL-C level was an independent determinant of in-stent large LRN on NIRS, a more aggressive lipid-lowering therapy may be necessary for patients with higher LDL-C undergoing PCI with stent implantation. Further prospective study is warranted to verify the clinical significance of NIRS-IVUS assessment for detecting large LRN in ISR lesions.

REFERENCES

1. Otsuka F, Vorpahl M, Nakano M, Foerst J, Newell JB, Sakakura K, Kutys R, Ladich E, Finn AV, Kolodgie FD, et al. Pathology of second-generation everolimus-eluting stents versus first-generation sirolimus- and paclitaxel-eluting stents in humans. *Circulation*. 2014;129:211–223. doi: 10.1161/CIRCULATIONAHA.113.001790

2. Cassese S, Byrne RA, Tada T, Pinieck S, Joner M, Ibrahim T, King LA, Fusaro M, Laugwitz KL, Kastrati A. Incidence and predictors of restenosis after coronary stenting in 10 004 patients with surveillance angiography. *Heart*. 2014;100:153–159. doi: 10.1136/heartjnl-2013-304933

3. Nakazawa G, Otsuka F, Nakano M, Vorpahl M, Yazdani SK, Ladich E, Kolodgie FD, Finn AV, Virmani R. The pathology of neoatherosclerosis in human coronary implants bare-metal and drug-eluting stents. *J Am Coll Cardiol*. 2011;57:1314–1322. doi: 10.1016/j.jacc.2011.01.011

4. Otsuka F, Byrne RA, Yahagi K, Mori H, Ladich E, Fowler DR, Kutys R, Xhepa E, Kastrati A, Virmani R, et al. Neoatherosclerosis: overview of histopathologic findings and implications for intravascular imaging assessment. *Eur Heart J*. 2015;36:2147–2159. doi: 10.1093/eurheartj/ehv205

5. Kuroda M, Otake H, Shinke T, Takaya T, Nakagawa M, Osue T, Taniguchi Y, Iwasaki M, Nishio R, Kinutani H, et al. The impact of in-stent neoatherosclerosis on long-term clinical outcomes: an observational study from the Kobe University Hospital optical coherence tomography registry. *EuroIntervention*. 2016;12:e1366–e1374. doi: 10.4244/EIJY15M12_05

6. Nakamura D, Dohi T, Ishihara T, Kikuchi A, Mori N, Yokoi K, Shiraki T, Mizote I, Mano T, Higuchi Y, et al. Predictors and outcomes of neoatherosclerosis in patients with in-stent restenosis. *EuroIntervention*. 2021;17:489–496. doi: 10.4244/EIJ-D-20-00539

7. Bezerra HG, Costa MA, Guagliumi G, Rollins AM, Simon DI. Intracoronary optical coherence tomography: a comprehensive review clinical and research applications. *JACC Cardiovasc Interv*. 2009;2:1035–1046. doi: 10.1016/j.jcin.2009.06.019

8. Yokoyama S, Takano M, Yamamoto M, Inami S, Sakai S, Okamatsu K, Okuni S, Seimiya K, Murakami D, Ohba T, et al. Extended follow-up by serial angioscopic observation for bare-metal stents in native coronary arteries: from healing response to atherosclerotic transformation of neointima. *Circ Cardiovasc Interv*. 2009;2:205–212. doi: 10.1161/CIRCINTERVENTIONS.109.854679

9. Gonzalo N, Serruys PW, Okamura T, van Beusekom HM, Garcia-Garcia HM, van Soest G, van der Giessen W, Regar E. Optical coherence tomography patterns of stent restenosis. *Am Heart J*. 2009;158:284–293. doi: 10.1016/j.ahj.2009.06.004

10. Lutter C, Mori H, Yahagi K, Ladich E, Joner M, Kutys R, Fowler D, Romero M, Narula J, Virmani R, et al. Histopathological differential diagnosis of optical coherence tomographic image interpretation after stenting. *JACC Cardiovasc Interv*. 2016;9:2511–2523. doi: 10.1016/j.jcin.2016.09.016

11. Gardner CM, Tan H, Hull EL, Lisauskas JB, Sum ST, Meese TM, Jiang C, Madden SP, Caplan JD, Burke AP, et al. Detection of lipid core coronary plaques in autopsy specimens with a novel catheter-based near-infrared spectroscopy system. *JACC Cardiovasc Imaging*. 2008;1:638–648. doi: 10.1016/j.jcmg.2008.06.001

12. Waxman S, Dixon SR, L'Allier P, Moses JW, Petersen JL, Cutlip D, Tardif JC, Nesto RW, Muller JE, Hendricks MJ, et al. In vivo validation of a catheter-based near-infrared spectroscopy system for detection of lipid core coronary plaques: initial results of the SPECTACL study. *JACC Cardiovasc Imaging*. 2009;2:858–868. doi: 10.1016/j.jcmg.2009.05.001

13. Nair A, Kuban BD, Tuzcu EM, Schoenhagen P, Nissen SE, Vince DG. Coronary plaque classification with intravascular ultrasound radiofrequency data analysis. *Circulation*. 2002;106:2200–2206. doi: 10.1161/01.CIR.0000035654.18341.5E

14. Waksman R, Di Mario C, Torguson R, Ali ZA, Singh V, Skinner WH, Artis AK, Cate TT, Powers E, Kim C, et al. Identification of patients and plaques vulnerable to future coronary events with near-infrared spectroscopy intravascular ultrasound imaging: a prospective, cohort study. *Lancet (London, England)*. 2019;394:1629–1637. doi: 10.1016/S0140-6736(19)31794-5

15. Ali ZA, Roleder T, Narula J, Mohanty BD, Baber U, Kovacic JC, Mintz GS, Otsuka F, Pan S, Virmani R, et al. Increased thin-cap neoatheroma and periprocedural myocardial infarction in drug-eluting stent restenosis: multimodality intravascular imaging of drug-eluting and bare-metal stents. *Circ Cardiovasc Interv*. 2013;6:507–517. doi: 10.1161/CIRCINTERVENTIONS.112.000248

16. Roleder T, Karimi Galougahi K, Chin CY, Bhatti NK, Brilakis E, Nazif TM, Kirtane AJ, Karmpaliotis D, Wojakowski W, Leon MB, et al. Utility of near-infrared spectroscopy for detection of thin-cap neoatherosclerosis. *Eur Heart J Cardiovasc Imaging*. 2017;18:663–669. doi: 10.1093/ehjci/jew198

17. Cutlip DE, Windecker S, Mehran R, Boam A, Cohen DJ, van Es GA, Steg PG, Morel MA, Mauri L, Vranckx P, et al. Clinical end points in coronary stent trials: a case for standardized definitions. *Circulation*. 2007;115:2344–2351. doi: 10.1161/CIRCULATIONAHA.106.685313

18. Yamamoto W, Fujii K, Otsuji S, Takiuchi S, Kakishita M, Shimatani Y, Hasegawa K, Ishibuchi K, Tamaru H, Ishii R, et al. Effect of neointimal tissue morphology on vascular response to balloon angioplasty in lesions with in-stent restenosis after drug-eluting stent deployment: an optical coherence tomography analysis. *Heart Vessels*. 2020;35:1193–1200. doi: 10.1007/s00380-020-01595-z

19. Madder RD, Goldstein JA, Madden SP, Puri R, Wolski K, Hendricks M, Sum ST, Kini A, Sharma S, Rizik D, et al. Detection by near-infrared spectroscopy of large lipid core plaques at culprit sites in patients with acute ST-segment elevation myocardial infarction. *JACC Cardiovasc Interv*. 2013;6:838–846. doi: 10.1016/j.jcin.2013.04.012

20. Takahashi N, Dohi T, Endo H, Takeuchi M, Doi S, Kato Y, Okai I, Iwata H, Okazaki S, Isoda K, et al. Coronary lipid-rich plaque characteristics in Japanese patients with acute coronary syndrome and stable angina: a near infrared spectroscopy and intravascular ultrasound study. *Int J Cardiol Heart Vasc*. 2021;33:100747. doi: 10.1016/j.ijcha.2021.100747

21. Erlinge D, Maehara A, Ben-Yehuda O, Bøtker HE, Maeng M, Kjøller-Hansen L, Engstrøm T, Matsumura M, Crowley A, Dressler O, et al. Identification of vulnerable plaques and patients by intracoronary near-infrared spectroscopy and ultrasound (PROSPECT II): a prospective natural history study. *Lancet*. 2021;397:985–995. doi: 10.1016/S0140-6736(21)00249-X

22. Zanchin C, Ueki Y, Losdat S, Fahrni G, Daemen J, Ondracek AS, Haner JD, Stortecky S, Otsuka T, Siontis GCM, et al. In vivo relationship between near-infrared spectroscopy-detected lipid-rich plaques and morphological plaque characteristics by optical coherence tomography and intravascular ultrasound: a multimodality intravascular imaging study. *Eur Heart J Cardiovasc Imaging*. 2021;22:824–834. doi: 10.1093/ehjci/jez318

23. Araki M, Yonetsu T, Lee T, Murai T, Kanaji Y, Usui E, Matsuda J, Hoshino M, Niida T, Hada M, et al. Relationship between optical coherence tomography-defined in-stent neoatherosclerosis and out-stent arterial remodeling assessed by serial intravascular ultrasound examinations in late and very late drug-eluting stent failure. *J Cardiol*. 2018;71:244–250. doi: 10.1016/j.jjcc.2017.09.005

24. Yabushita H, Bouma BE, Houser SL, Aretz HT, Jang IK, Schlendorf KH, Kauffman CR, Shishkov M, Kang DH, Halpern EF, et al. Characterization of human atherosclerosis by optical coherence tomography. *Circulation*. 2002;106:1640–1645. doi: 10.1161/01.CIR.0000029927.92825.F6

25. Tsujita K, Sugiyama S, Sumida H, Shimomura H, Yamashita T, Yamanaga K, Komura N, Sakamoto K, Oka H, Nakao K, et al. Impact of dual lipid-lowering strategy with ezetimibe and atorvastatin on coronary plaque regression in patients with percutaneous coronary intervention: the multicenter randomized controlled PRECISE-IVUS trial. *J Am Coll Cardiol*. 2015;66:495–507. doi: 10.1016/j.jacc.2015.05.065

26. O'Keefe JH Jr, Cordain L, Harris WH, Moe RM, Vogel R. Optimal low-density lipoprotein is 50 to 70 mg/dl: lower is better and physiologically normal. *J Am Coll Cardiol*. 2004;43:2142–2146. doi: 10.1016/j.jacc.2004.03.046

27. Ota H, Omori H, Kawasaki M, Hirakawa A, Matsuo H. Clinical impact of PCSK9 inhibitor on stabilization and regression of lipid-rich coronary plaques: a near-infrared spectroscopy study. *Eur Heart J Cardiovasc Imaging*. 2022;28:217–228.

28. Jang JY, Kim JS, Shin DH, Kim BK, Ko YG, Choi D, Jang Y, Hong MK. Favorable effect of optimal lipid-lowering therapy on neointimal tissue characteristics after drug-eluting stent implantation: qualitative optical coherence tomographic analysis. *Atherosclerosis*. 2015;242:553–559. doi: 10.1016/j.atherosclerosis.2015.08.014

29. Madder RD, Khan M, Husaini M, Chi M, Dionne S, van Oosterhout S, Borgman A, Collins JS, Jacoby M. Combined near-infrared spectroscopy and intravascular ultrasound imaging of pre-existing coronary

artery stents: can near-infrared spectroscopy reliably detect neoatherosclerosis? *Circ Cardiovasc Imaging*. 2016;9:e003576. doi: 10.1161/CIRCIMAGING.115.003576

30. Tearney GJ, Regar E, Akasaka T, Adriaenssens T, Barlis P, Bezerra HG, Bouma B, Bruining N, Cho JM, Chowdhary S, et al. Consensus standards for acquisition, measurement, and reporting of intravascular optical coherence tomography studies: a report from the international working Group for Intravascular Optical Coherence Tomography Standardization and Validation. *J Am Coll Cardiol*. 2012;59:1058–1072. doi: 10.1016/j.jacc.2011.09.079

31. Fujii K, Kubo T, Otake H, Nakazawa G, Sonoda S, Hibi K, Shinke T, Kobayashi Y, Ikari Y, Akasaka T. Expert consensus statement for quantitative measurement and morphological assessment of optical coherence tomography. *Cardiovasc Interv Ther*. 2020;35:13–18. doi: 10.1007/s12928-019-00626-5

32. Mintz GS, Nissen SE, Anderson WD, Bailey SR, Erbel R, Fitzgerald PJ, Pinto FJ, Rosenfield K, Siegel RJ, Tuzcu EM, et al. American College of Cardiology clinical expert consensus document on standards for acquisition, measurement and reporting of intravascular ultrasound studies (IVUS). *J Am Coll Cardiol*. 2001;37:1478–1492. doi: 10.1016/S0735-1097(01)01175-5

33. Saito Y, Kobayashi Y, Fujii K, Sonoda S, Tsujita K, Hibi K, Morino Y, Okura H, Ikari Y, Honye J. Clinical expert consensus document on standards for measurements and assessment of intravascular ultrasound from the Japanese Association of Cardiovascular Intervention and Therapeutics. *Cardiovasc Interv Ther*. 2020;35:1–12. doi: 10.1007/s12928-019-00625-6

34. Suzuki N, Asano T, Nakazawa G, Aoki J, Tanabe K, Hibi K, Ikari Y, Kozuma K. Clinical expert consensus document on quantitative coronary angiography from the Japanese Association of Cardiovascular Intervention and Therapeutics. *Cardiovasc Interv Ther*. 2020;35:105–116. doi: 10.1007/s12928-020-00653-7

Supplemental Material

Data S1.

Supplemental Methods

OCT/OFDI acquisition and imaging analysis

The tip of the OCT/OFDI lens was placed 10 mm distal to the distal edge or as far as the starting point of the pullback distal to the stent. Appropriate acquisition of OCT/OFDI images required continuous intracoronary injection of 12-16 ml contrast or low molecular weight dextran at a speed of 3-4 ml/s followed by catheter pullback (20 mm/s).

Quantitative and qualitative analysis of OCT/OFDI was performed based on previously validated criteria. [31, 32] The OCT/OFDI images were analyzed offline in each cross-section selected at 1 mm longitudinal steps throughout the pullback from the distal to the proximal stent edge. The neointima was defined as the tissue between the luminal contour and stent contour. The neointimal hyperplasia (NIH) area (stent area–lumen area) and percent NIH "[(NIH area/stent area) × 100]" were calculated. [1] In the present study, we used the following classification of four patterns of OCT/OFDI findings. A) homogeneous neointima pattern was defined as signal-rich regions with low attenuation which reflects smooth muscle cells or collagen rich neointima. B)

heterogeneous with layered neointima pattern was defined as one with layers having

different optical properties (i.e., an adluminal high-scattering layer and an abluminal

low-scattering layer) which reflect layer of loose neointimal tissue with

neovascularization and inflammation close to stent struts and a smooth muscle cell rich

neointimal layer toward the lumen. C) heterogeneous without layered neointima pattern,

defined as one with focally changing optical properties with low attenuation, which

reflect stent-induced hypersensitivity vasculitis or proteoglycan rich neointima. D)

neoatherosclerosis (NA) pattern was defined as a signal-poor region with diffuse

borders, which reflect the involvement of atherogenic progression within neointima.

Similar to the characteristics of arteriosclerosis in the native coronary arteries, NA has

the pathological characteristics such as (i) early foamy macrophage infiltration, (ii)

manifest atherosclerotic plaque development, and (iii) necrotic core plaque formation

with or without thin fibrous caps. [3, 10]

NIRS-IVUS acquisition and imaging analysis

The NIRS-IVUS imaging was performed after OCT/OFDI image acquisition and

after intracoronary administration of 0.2 mg nitroglycerin into the stented artery. The

NIRS-IVUS catheter was positioned 10 mm distal to the stent or as far distal to it as

possible distal if it could not be delivered distal to the stent. Automated pullback was started at a speed of 0.5 mm/s with ~80 spectroscopic measurements performed per minute. NIRS estimates the distribution of lipids within the neointima and presents the data as red or yellow on the NIRS chemogram, with yellow indicating the presence of lipids and red the absence. The NIRS chemogram allows calculation of the lipid core burden index, a measure of the total lipid burden (total yellow pixels/total viable pixel within the region of interest × 1000).

Quantitative IVUS analyses were performed according to the previously validated criteria. [33, 34] The lumen, stent, and vessel were assessed and measured every 0.5 mm. Parameters assessed included lumen area, stent area, vessel area, and NIH area. The value of % NIH was calculated the same as was done for definitions of OCT/OFDI.

Co-registration of NIRS-IVUS with OCT/OFDI

Anatomical landmarks were set as the proximal and distal edges of the stent. Based on these landmarks, we matched the NIRS chemogram with the corresponding cross-sectional images of OCT/OFDI. To compare the distribution of lipids on the NIRS chemogram with OCT/OFDI, we analyzed the $maxLCBI_{4mm}$ corresponding with culprit segments diagnosed by OCT/OFDI. In addition, we assessed the correlation between

LCBI values on NIRS and neointima characteristics on OCT/OFDI findings.

Quantitative coronary angiographic analysis

Angiographic measurements were performed with QAngio XA software (Medis, Leiden, The Netherlands). Images were selected with an end-diastolic cine frame of the most severe and non-foreshortened projection. The reference lumen diameter, the minimal lumen diameter, the percentage of diameter stenosis, and the length of the lesion were measured. [35]

Table S1. Lesion, angiographic, and imaging characteristics of lesions.

	Overall n=64	Large LRN n=21	Non-large LRN n=43	*p* value
Lesion characteristics				
Lesion location				0.42
RCA, n (%)	18 (28.1)	7 (33.3)	11 (25.6)	
LAD, n (%)	33 (51.6)	10 (47.6)	23 (53.5)	
LCx, n (%)	13 (20.3)	4 (19.1)	9 (20.9)	
Quantitative coronary angiography				
Diameter of stenosis, %	71.8 ± 14.6	73.7 ± 16.8	70.9 ± 13.6	0.47
Minimum lumen diameter, mm	0.7 ± 0.4	0.6 ± 0.4	0.8 ± 0.4	0.05
Reference lumen diameter, mm	2.4 ± 0.5	2.4 ± 0.4	2.5 ± 0.6	0.31
Lesion length, mm	26.4 ± 10.9	28.6 ± 13.1	25.4 ± 9.7	0.27
OCT/OFDI findings				
Quantitative analysis				
Minimal fibrous cap thickness, μm	115 [56, 180]	130 [56, 171]	109 [83, 184]	0.97
NA with fibrous cap thickness <65 μm, n (%)	11 (31.4)	8 (44.4)	3 (17.7)	0.15
Qualitative analysis				
Rupture, n (%)	7 (10.9)	4 (19.1)	3 (6.7)	0.2
Thrombi, n (%)	4 (6.3)	3 (14.3)	1 (2.3)	0.1
Neovascularization, n (%)	9 (14.1)	2 (9.5)	7 (16.3)	0.71
Intrastent calcification, n (%)	18 (28.1)	5 (23.8)	13 (30.2)	0.77

LAD, left anterior descending brunch; LCx, left circumflex artery; LRN, lipid-rich neointima; NA, neoatherosclerosis; RCA, right coronary artery

Table S2. Best cut-off values of NIRS, OCT/OFDI, and IVUS plaque characteristics for predicting NA.

	AUC (95% CI)	Cut-off	Sensitivity	Specificity	PPV	NPV	*p* value
NIRS							
MaxLCBI$_{4mm}$	0.92 (0.83-1.00)	405	0.94	0.91	0.80	0.98	<0.001
OCT/OFDI							
Max lipid arc, °	0.80 (0.65-0.94)	218	0.88	0.61	0.68	0.85	0.001
IVUS							
Percent NIH (at MLA site), %	0.57 (0.40-0.74)	84.8	0.18	1.0	1.0	0.23	0.42

AUC, area under curve; CI, confidence interval; IVUS, intravascular ultrasound; LCBI, lipid core burden index; MLA, minimal lumen area; NA, neoatherosclerosis; NIH, neointima hyperplasia; NIRS, near-infrared spectroscopy, NPV, negative predictive value; OCT, optical coherence tomography; OFDI, optical frequency domain system; confidence interval; PPV, positive predictive value